SIMULATION STUDY OF SPONTANEOUS IMBIBITION

by
Douglas Ruth
University of Manitoba, Winnipeg, Manitoba, Canada
Norman Morrow and Li Yu
Department of Chemical and Petroleum Engineering
University of Wyoming, Laramie, Wyoming, USA
Jill Buckley
Petroleum Recovery Research Center, Socorro, New Mexico, USA

Abstract
Imbibition is an important phenomenon in many displacement processes. In particular, the transfer of liquids between fissures and the matrix in fractured reservoirs is dominated by imbibition. Re-examination of published results and new experimental data has resulted in a modified version of the Mattax and Kyte time-scaling that includes variations in water-oil viscosity ratio, sample shape, and boundary conditions. The resulting semi-empirical scaling group can be compared with simulations based on the mechanics of two-phase flow with capillary pressure as the driving force. This paper presents the results of a simulation study of one-dimensional, counter-current imbibition in a strongly water-wet sample.

As a first step, the generalized correlation for production was history-matched using core and fluid properties for which imbibition results have been reported. Initial water saturation was assumed to be zero. A logarithmic form was assumed for the capillary pressure curve and Corey equations were assumed for the relative permeability curves. A close match of oil recovery was obtained between the experimental data and the simulated imbibition. The core and fluid properties were systematically modified to test sensitivities. Variations in permeability, porosity, sample length and diameter, and interfacial tension were scaled exactly by the simulation. For oil viscosities in the range covered by the experimental data, agreement was good but not exact. The study was then extended to investigate the effects of varying capillary pressure curve shape, relative permeability, and initial water saturation, properties not explicitly included in the scaling group. For these simulations, the basic shapes of the oil-production-versus-time curves were essentially preserved. Overall agreement with the correlation was satisfactory. The initial water saturation was varied between 0% and 30% and the production curves were normalized with respect to the mobile oil saturation. Saturation profiles are presented which illustrate the simulated effect of initial water saturation on the imbibition process.

Introduction
Displacement of oil by spontaneous imbibition of water can be the dominant recovery mechanism in low permeability, fractured reservoirs which are water-wet (Aronofsky et al., 1958; Warren and Root, 1963; Kazemi, et al., 1992). Spontaneous imbibition is driven by the surface energy of the reservoir. Imbibition is a highly nonlinear process and conditions under which the process can be scaled are still being explored.

Scaling laws developed by Rapoport (1955) were applied by Mattax and Kyte (1962) to the problem of oil recovery by spontaneous imbibition. The conditions under which the scaling law was applicable were very restrictive. Necessary conditions included negligible influence of gravity forces, identical sample shapes, boundary conditions, oil/water viscosity ratio, initial fluid saturations, and directly proportional capillary pressure relationships. Re-examination of published results (Mattax and Kyte, 1962; Hamon and Vidal, 1986) and additional experimental results lead to a semi-empirical scaling group (Ma et al. 1997). The following fit to an Aronofsky model will be referred to as the correlation:

$$\frac{R}{R_\infty} = 1 - \frac{1}{(1 + 0.04 t_D)^{1.5}}$$

where R is the recovery, R_∞ is the ultimate recovery, and

$$t_D = t\sqrt{\frac{k}{f}}\,\frac{s}{L_C^2\sqrt{m_w m_o}}.$$

Here t is time, k is permeability, f is porosity, s is interfacial tension, L_C is a geometrical scaling factor (in the current paper simply the length of the sample L_C, m_w is the water viscosity, and m_o is the oil viscosity.

The scaled results apply to very strongly water-wet media with zero initial water saturation. Changes in imbibition rate with initial water saturation at strongly water-wet conditions have also been reported (Viksund et al 1998). The resulting semi-empirical scaling groups and relative trends in imbibition rate with changes in initial water saturations provide a body of data that can be tested against simulations using the basic principles of two-phase flow. Blair (1964) stressed the value of using simulation to investigate imbibition phenomena and the need to test results against experiments. The difference with respect to standard simulations of two-phase flow is that capillary pressure rather then an imposed pressure gradient provides the driving force.

The first step in the simulation is to show that the experimental results can be matched using measured or otherwise realistic values of input data. Parameters that are included in the scaling group and other parameters such as the relative permeabilities of each phase can then be varied independently, to identify trends in imbibition behavior. The results are compared with experimental results for ranges of parameters covered by the experimental data.

Formulation of the Numerical Simulator

The simulator is based on a conventional, explicit, finite-difference scheme. The software program was developed by modifying a commercially available numerical code that is normally used to simulate forced displacement (injection of water to displace oil). The program was already designed to handle potential imbibition at the production face. The modifications, designed to simulate the case of a cylindrical core with one end open, were minor and consisted of setting the injected flow to zero and removing mathematical problems (zero divides) that resulted. Two features of the simulator allow simulation of imbibition processes:

1. The differencing scheme is "upstream." With reference to Figure 1, this means that the properties at the grid boundaries are taken to be the properties of the cell from which the fluid (either oil or water) is flowing. Because the flow is countercurrent, this means that oil-flow at a grid boundary is governed by properties to the left of the boundary while water-flow is governed by properties to the right of the boundary. There is nothing unique about this scheme; it is standard in many numerical simulators.
2. The properties of the imbibition face (the end of the sample that is exposed to water) are determined by assuming that that face is fully contacted by water, that is, that the capillary pressure is zero. This results in the maximum water relative permeability (the upstream direction for the water at the sample face is outside the sample) and the minimum capillary pressure. In the simulator, the driving force is the difference in the capillary pressure between the outside face and the first grid block. Because the grid block at the inlet face is originally at zero water saturation, this driving force is maximum at the beginning of the simulation.

Test Parameter Specifications

The present study uses a base-case system of parameters as listed in Table 1. The parameters f, k, S_{wr}, and S_{or} are typical experimental values for Berea sandstone core. The relative permeabilities were assumed as Corey (1955) functions,

$$k_{ro} = k_{roe}\left(\frac{S_o - S_{ro}}{1 - S_{ro}}\right)^{n_o}$$

and

$$k_{rw} = k_{rwe}\left(\frac{S_w}{1-S_{ro}}\right)^{n_w}$$

with the end-point oil relative permeability set to 1.0. The capillary pressure curve was assumed to be logarithmic in form, and related to the threshold pressure by

$$Pc = Pc_t\left[1 - B\ln\left(\frac{S_w}{1-S_{ro}}\right)\right]$$

with the $S_w = 1 - S_{ro}$ value given by the Leverett J-Function (1941) formulation

$$Pc_t = J\cos(q)\sqrt{\frac{k}{f}}$$

with $J = 0.15$.

Table 1 The Test Parameters

Variable	Value	Units	Variable	Value	Units
f	0.215	-	k	600.0	mD
L	5.08	cm	D	3.18	cm
m_o	0.97	cp	m_w	0.97	cp
k_{roe}	1.0	-	k_{rwe}	0.04	-
n_o	1.756	-	n_w	2.018	-
S_{or}	0.43	-	S_{wi}	0.0	-
s	50.0	dynes/cm	B	5.255	-
Pc_t	2.29	kPa			

Base case viscosities for oil and water were both set at 0.97 cp. The core dimensions are typical of the laboratory samples. The first step in the study was to predict recovery versus time by applying the test parameter specifications to the correlation. Therefore, relative permeability and capillary pressure curves were chosen by setting $k_{rwe} = 0.04$ (Braun and Holland, 1995) and optimizing values of n_o, n_w and the capillary pressure curve shape (B). The resultant values, included in Table 1, gave the curves shown in Figure 2. These curves are typical of experimental data for Berea sandstone.

Productions predicted by the simulator for this base case, and by the correlation, are compared in Figure 3a. This figure uses linear scales. Differences in the early time results between the simulation and the correlation for this base case simulation are apparent from the plots of recovery versus log t_D shown in Figure 3b.

Inspection of experimental data from which the correlation was developed indicates that the early time differences could be reduced by modifying the one parameter Aronofsky equation (1958) used as a mathematical model of the correlation. An example of an improved one-parameter fit to the correlated recovery for late time data was used by Viksund et al 1998. Obviously an improved fit to the data could be obtained by increasing the number of fitting parameters. However, the early time differences may also be related to the time needed for water to establish imbibition paths within the rock. The simulator assumes that this will occur immediately. Furthermore, collection of oil that is recorded as production may be delayed if the displaced oil clings to the rock surface. However, for most practical purposes, the differences in the early time results is not important. These differences were observed for all simulations. The aim of the present study is to determine which of the mechanisms that influence imbibition are

important, and to test the scaling group both within and outside the range of experimental data. Therefore, the sensitivity of the simulated results to various parameters will be presented with respect to the base case.

Testing Parameters in the Scaling Law

The second stage in the study was to vary systematically the parameters that appear in the scaling law (k, f, s, L, m_o and m_w) and determine the amount by which the resulting simulated results deviated from the base-case-simulation. Not surprisingly, several of these parameters had no effect, giving results, which duplicated the base-case. These parameters were $k, f, L,$ and s. The values of k tested ranged from 0.6 mD to 6000 mD and f from 0.05 to 0.25. L and s were each changed by a factor of 2. These results provided confirmation that the performance of the simulator is as expected.

A feature of the scaling group that is of special interest is the correlation of experimental results by the geometric mean of the oil and water viscosities. In experimental studies, the value of m_o was varied from 0.97 to 156cp (Ma et al. 1999). There is close agreement between the base case and the simulated results for variations in m_o in this range (see Figure 4a). The results are consistent with simulations of imbibition reported by Blair (1964) for input data of significantly different character (for example imbibition capillary pressure that decreased continuously to zero at residual oil, and about one order of magnitude higher end point relative permeabilities to water) from those of the base case. From Figure 5a it is seen that there is divergence from the base case at later times. However, detailed inspection of the original data (Ma et al. 1999) for recovery of viscous oil did not provide any indication of this trend. When the values of m_o were varied over 5 orders of magnitude, 0.01 to 1000, the dimensionless time predicted for displacement of low viscosity non-wetting phase is significantly longer than for the base case (Fig. 4b).

The last parameter tested was m_w. Preliminary experimental data showed little effect of wetting phase viscosity for m_w 0.1 to 15cp. Varying m_w in the simulation from 0.97 to 15cp also showed little deviation from the base case.

Experiments on displacement of gas ($m_g \cong 0.02$ cp) by imbibition of oil (oil is now the wetting phase) with viscosities in the range 1 to 162 cp gave dimensionless times for imbibition that were much larger than predicted by the scaling group (Wang, 1999). The results of simulations with μ_o in the range 1 – 162cp and a non-wetting phase of 0.02cp exhibited the same trends as the experiments (Figure 5). However, the rate of imbibition will have been affected by compressibility of the gas phase in the experiments and this is not taken into account in the version of the simulator used in the present study. This aspect of fluid properties and imbibition will be the subject of further study.

Testing Parameters Not Included in the Scaling Law

A remarkable aspect of the scaling law is that many parameters such as the shape and end-point values of the relative permeabilities and the shape of the capillary pressure curve, that can be expected to affect the displacement processes, are not explicitly included in the correlation. As a test of their effect, variations in the relative permeability and capillary pressure curves were simulated.

Capillary Pressure

Figure 6 shows the effect of varying capillary pressure curve shape as expressed by B. Figure 6a shows the capillary pressure curves considered and Figure 6b the resulting production curves. The values of B used were 2.62, 3.93, 5.26 (base case), 6.55, and 7.86. The capillary pressure curve shape clearly has a systematic effect on the production. This is not surprising because the shape of the curve controls the magnitudes of Pc; it is the difference in capillary pressure that determines the flow rate. However, with changes in B of almost a factor of 4, the change in t_D is less than one order of magnitude.

Relative Permeability

Figure 7 shows the effect of varying the end-point relative permeability, k_{rwe}, of the water phase. Here the tested values of k_{rwe} were 0.02, 0.04 (base case), 0.08, 0.16, and 0.32. The simulated curves deviate from the base curve by about an order of magnitude for a 16-fold variation in k_{rwe}. For water-wet rocks such as Berea, the endpoint relative permeability to water should remain low. From one half to double the base case of $k_{rwe} = 0.04$ the variation from the base case is minor.

Figure 8 shows the effect of varying the shape of the water relative permeability curve. The values of the exponent n_w were 1.1, 1.756 (base case), 3.0, 4.0, and 5.0. For high values of n_w the disagreement with the scaling law is apparent. However, the variation is less than an order of magnitude, even for this extreme range of shapes. Values of n_w as high as 5.0 are well removed from the shape of water phase relative permeabilities for Berea sandstone.

Figure 9 shows the effect of varying the shape of the relative permeability curve to oil. The values of n_o were 1.1, 2.018 (base case), 3.0, 4.0, and 5.0. The results group around the base case results. There is a systematic increase in t_D with n_o that is accentuated at higher values of n_o and later times, and is obviously related to the extremely low permeabilities to oil as the water saturation increases.

In summary, there are no major inconsistencies between the correlation derived from experimental data and simulations that result from parametric variations of the base case. Furthermore, many of the changes in one parameter, for example changing one relative permeability without affecting the other, may not be physically reasonable. There may well be compensating effects that contribute to the success of the scaling group such as, for example the mobility conditions for two phase counter-current flow.

Initial Water Saturation

The effect of initial water saturation on imbibition rate is of special practical interest and has been investigated by experiment for Berea sandstone and chalk (Viksund et al. 1998). Figure 10 shows the simulated effect of initial water saturation. The saturations considered were 0.0, 0.05, 0.1, 0.2, and 0.3. The decrease in dimensionless time for imbibition is qualitatively similar to that measured by Viksund et al (1998) for chalk (very low permeability). The behavior measured for Berea sandstone is more complicated (Viksund et al., 1998). The dimensionless time for imbibition increased by a factor of about 8 with increase in initial saturation up to 7%, stayed close to constant up to 14%, and then decreased. The trend of decrease in t_D with increase in S_{wi} above 14% agrees with the trend predicted by simulation, but unlike chalk, the dimensionless time for imbibition into Berea sandstone is always longer than that for the correlation developed for $S_{wi} = 0$.

The simulator can also predict water saturation profiles. Figure 11 shows the profiles for the base case. Generally, the water advances from the invading face as a wedge in saturation until it reaches the closed end of the sample. The saturation in the first grid block (the imbibition-end of the sample) obviously cannot go to residual oil because under counter current flow conditions, a significant mobile oil saturation must remain for oil to exit the sample. Figure 12 shows water saturations for the case of an initial water saturation of 10%. The shapes of the curves are very similar to the base case, except that the base line is at 10% saturation rather then zero.

Concluding Remarks

The results of simulations presented in this paper provide useful guidance to further experimental studies. In situ saturation measurement techniques can provide saturation profiles (Graue & Viksund, 1994) which can then be tested against simulation. Experimental micromodel studies of the imbibition mechanisms, and theoretical network modeling (such as those reported by Blunt, 1997 and Dixit, et al 1999) will also contribute to further understanding of the imbibition problem.

Conclusions

1. The simulation study provides substantial agreement with predictions from a correlation based on experimental data. Within the ranges of parameters used in the experiments, agreement between the model and simulated results is very close.
2. Predictions can be made of the effect on imbibition of variation of parameters that were held constant in the original development of the basic scaling laws.
3. Over the range of viscosity ratios tested by experiment the correlation based on the geometric mean of the viscosity ratios was in close agreement with the simulated effect of viscosity ratio.
4. Trends predicted by simulation for very high viscosity ratios given by using a very low viscosity non-wetting fluid (gas) were qualitatively consistent with experimental results.
5. Changes in imbibition rate with initial water saturation predicted by simulation were similar to trends exhibited by experimental results.

References

Aronofsky, J.S., Masse, L. and Natanson, S.G.: "A Model for the Mechanism of Oil Recovery for the Porous Matrix Due to Water Invasion in Fractured Reservoirs," *Trans. AIME,* 213, p.17, 1958.

Blair, P.M.: "Calculation of Oil Displacements by Countercurrent Water Imbibition" *SPEJ*, p. 195-202, Sept. 1964.

Blunt, M.J.: "Pore Level Modeling of the Effects of Wettability," SPEJ, 2, (December), p.494-510, 1997.

Braun, E.M. and Holland, R.F.: "Relative Permeability Hysteresis: Laboratory Measurements and a Conceptual Model," *SPERE*, p. 222-8, Aug. 1995.

Corey, A.T: "The Interrelation Between Gas and Oil Relative Permeabilities", *Producers Monthly*. p. 38-41, Nov 1954.

Dixit, A.B., McDougall, S.R., Sorbie, K.S., and Buckley, J.S.: "Pore Scale Modelling of Wettability Effects and their Influence on Oil Recovery," *SPEREE*, 2, (February), p.25-36, 1999.

Graue, A. and Viksund, B.G.: "Imaging Immiscible Two Phase Flow in Low Permeability Chalk Emphasis on Recovery Mechanisms and Scaling," *EAPG/AAPG Special Conference on Chalk*, Copenhagen, Sept. 7-9, 1994.

Hamon, G. and Vidal, J.V.: "Scaling-up the Capillary Imbibition Process from Laboratory Experiments on Homogeneous and Heterogeneous Samples," *SPE 15852*, the European Petr. Conf., London, Oct. 20-22, 1986.

Kazemi, H. Gilman, J.R., and Eisharkawy, A.M.: "Analytical and Numerical Solution of Oil Recovery from Fractured Reservoirs with Empirical Transfer Function," *SPERE,* p. 219-27, May 1992.

Leverett, M.C.: "Capillary Behavior in Porous Solids", *Trans. AIME*, 142, p. 152, 1941.

Ma, S., Morrow, N.R. and Zhang, X.: "Generalized Scaling of Spontaneous Imbibition Data for Strongly Water-Wet Systems", *JPSE,* 18, p. 165-178, 1997.

Ma, S., Zhang, X., and Morrow, N.R.: "Influence of Fluid Viscosity on Mass Transfer Between Rock Matrix and Fractures," *JCPT*, 38, 7, p. 25-30, July 1999.

Mattax, C.C. and Kyte, J.R.: "Imbibition Oil Recovery From Fractured, Waterdrive Reservoirs," *SPEJ,* June, p.177, 1962.

Rapoport, L.A.: "Scaling laws for use in design and operation of water-oil flow models" *Trans. AIME* 204, p. 143-150, 1955.

Viksund, B.G., Morrow, N.R., Ma, S., Wang, W., and Graue, A.: "Initial Water Saturation and Oil Recovery from Chalk and Sandstone by Spontaneous Imbibition", *Proceedings of the International Symposium of the Society of Core Analysts*, The Hague, September 14-16, 1998.

Wang, R.: " Gas Recovery from Porous Media by Spontaneous Imbibition of Liquid," Univ. of Wyoming Masters Thesis, December, 1999.

Warren, J.E. and Root, P.J., "The Behavior of Naturally Fractured Reservoirs", *SPEJ,* p. 245-255, September, 1963.

Acknowledgements

Support for this work was provided by the National Science and Engineering Research Council of Canada, ARCO, British Petroleum/Amoco, Chevron, ELF/Total/Gas de France/IFP, JNOC, Phillips, Shell, Statoil, The Enhanced Oil Recovery Institute of the University of Wyoming, and the National Technology Office Partnership of the U.S. Department of Energy.

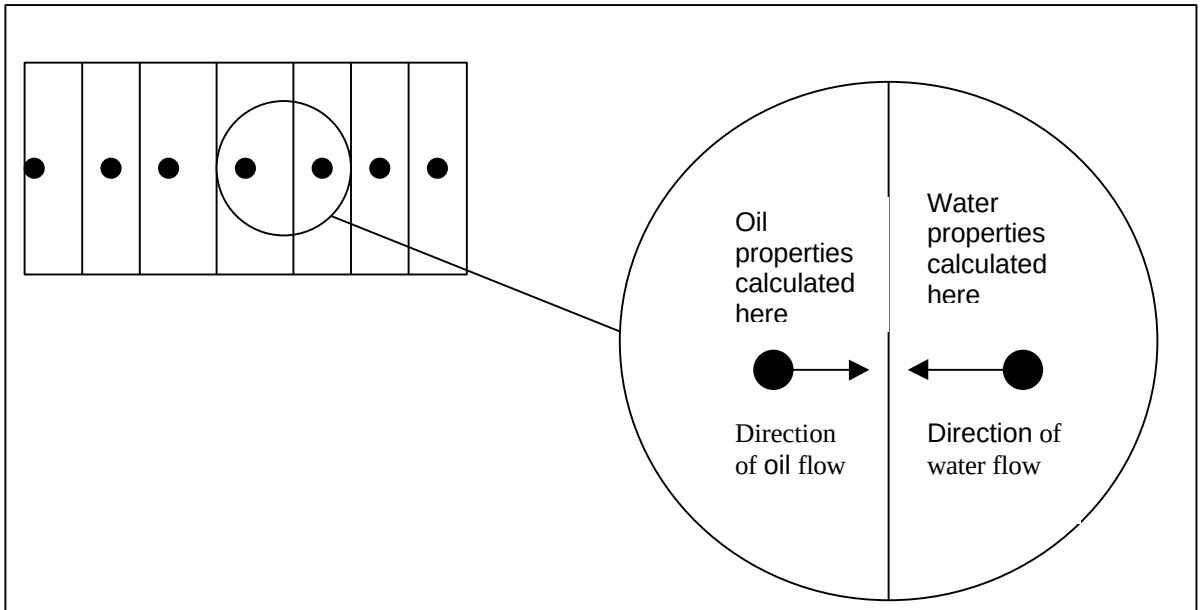

Figure 1 The Upstream Differencing Scheme

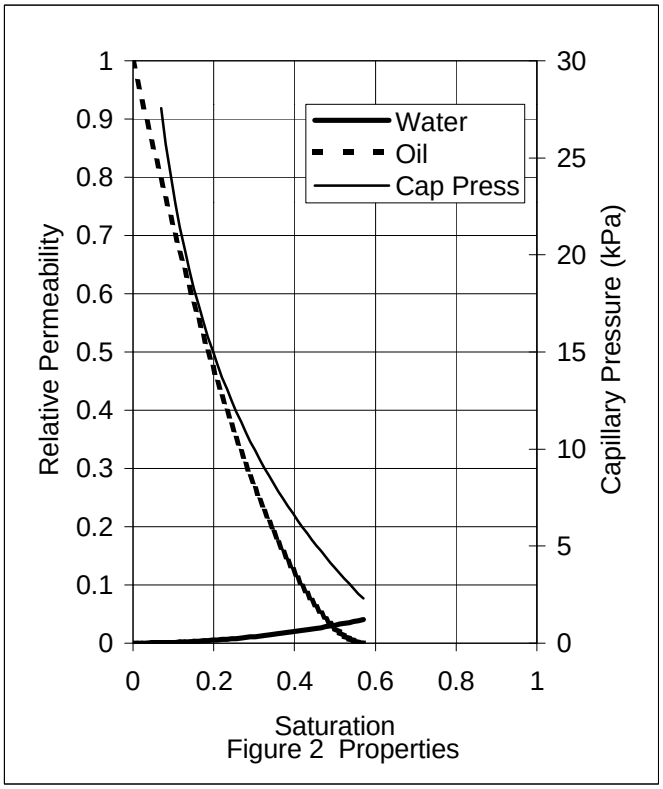

Figure 2 Properties

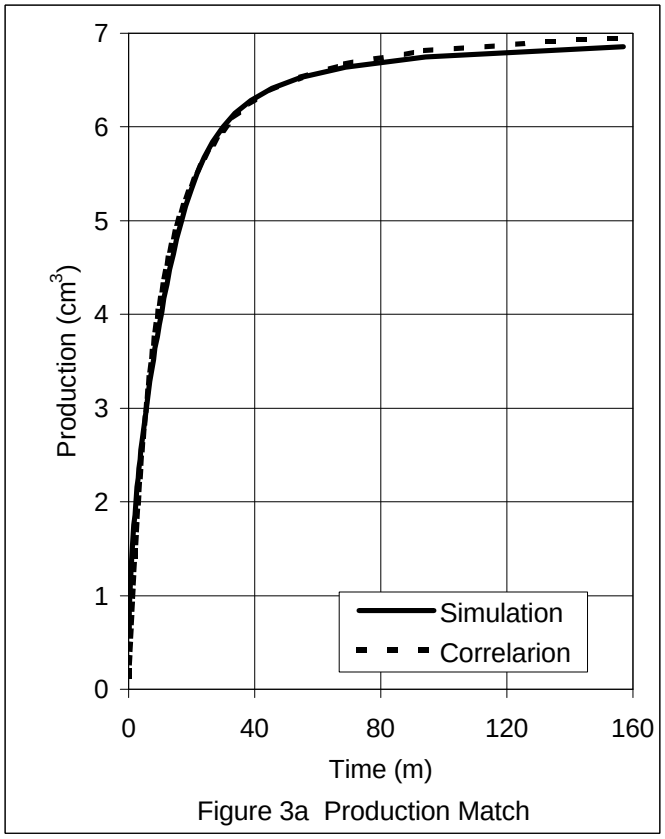

Figure 3a Production Match

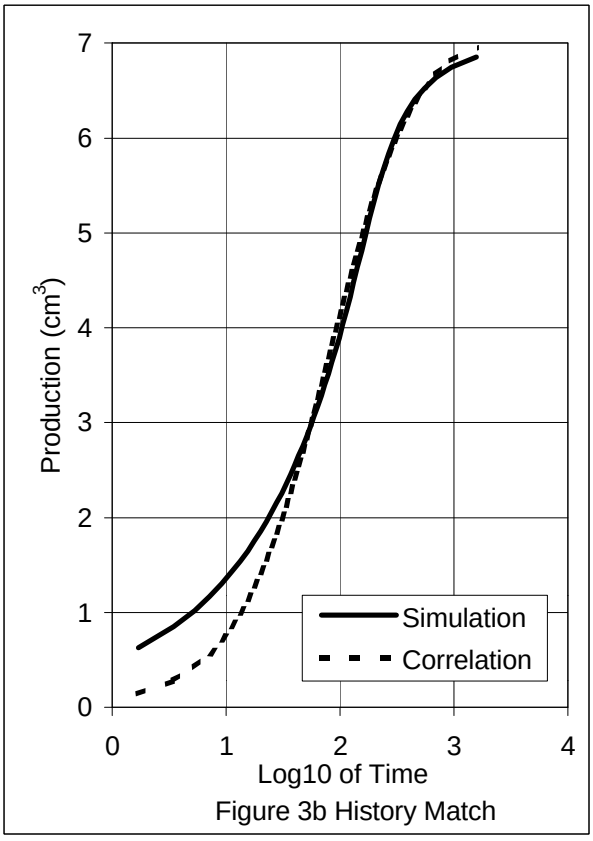

Figure 3b History Match

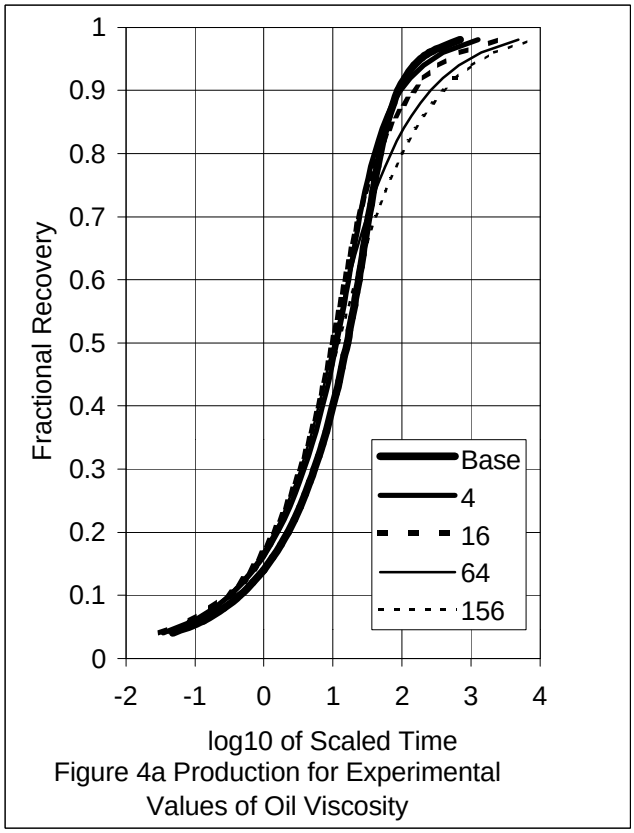

Figure 4a Production for Experimental Values of Oil Viscosity

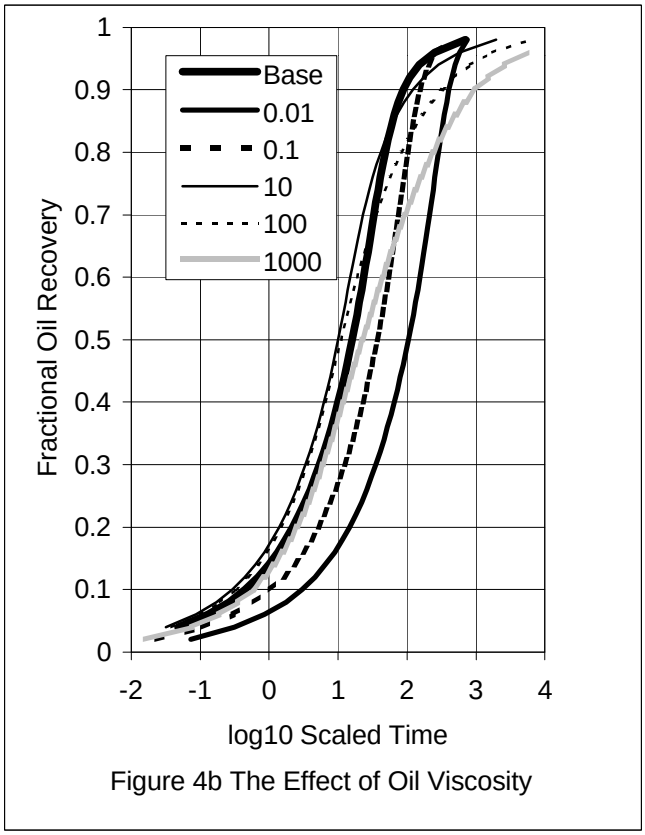

Figure 4b The Effect of Oil Viscosity

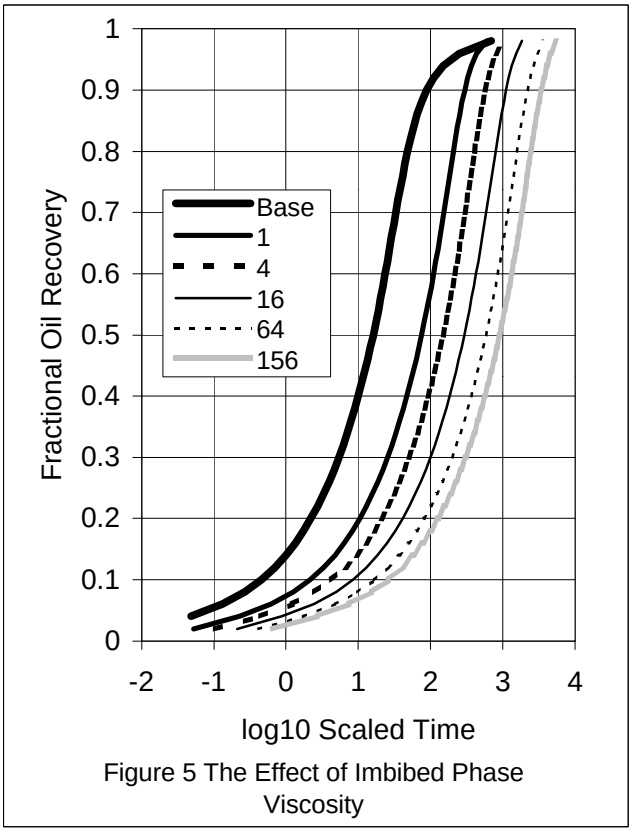

Figure 5 The Effect of Imbibed Phase Viscosity

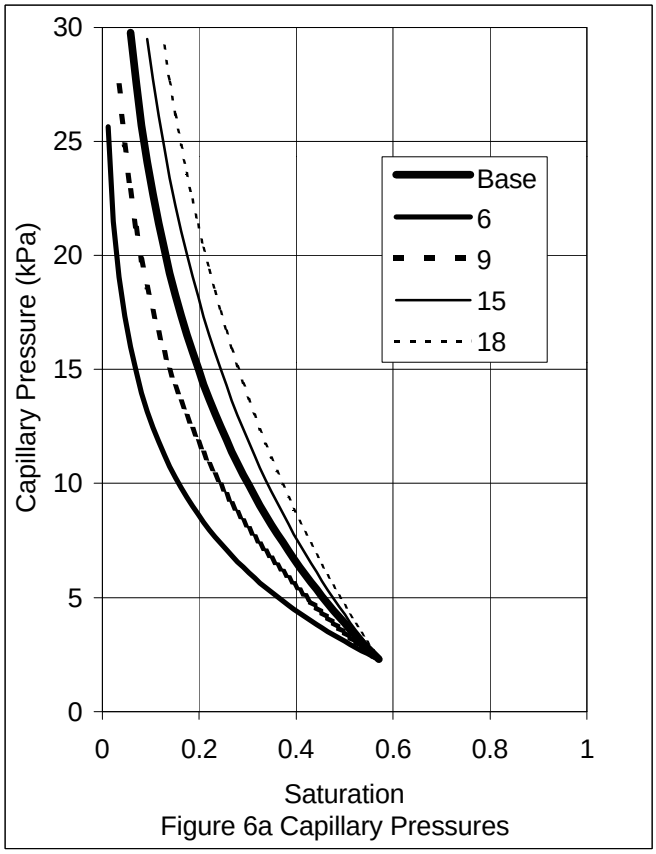

Figure 6a Capillary Pressures

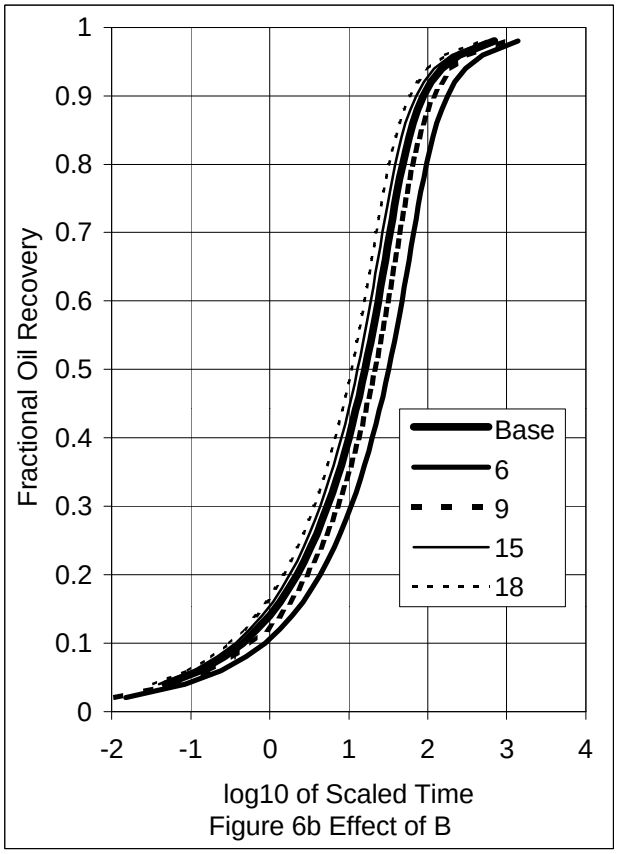

Figure 6b Effect of B

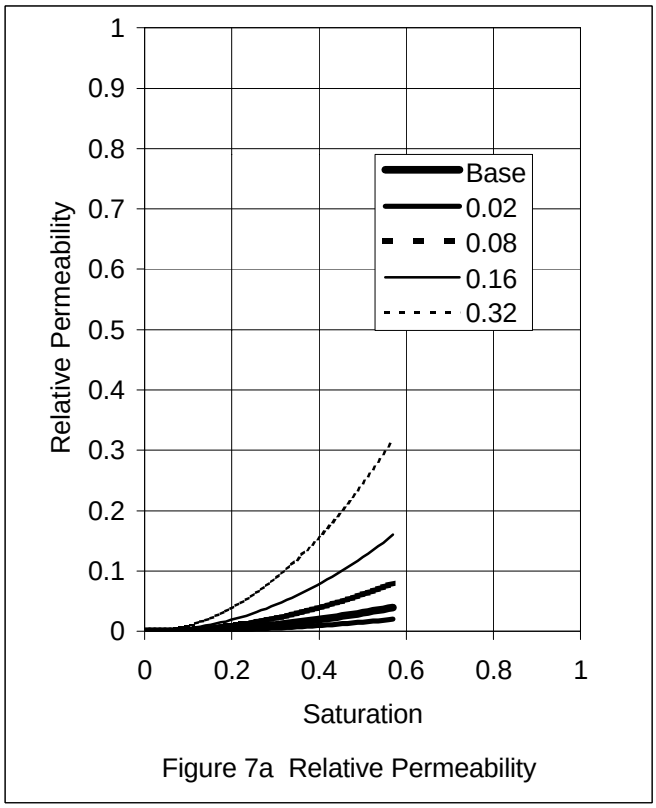

Figure 7a Relative Permeability

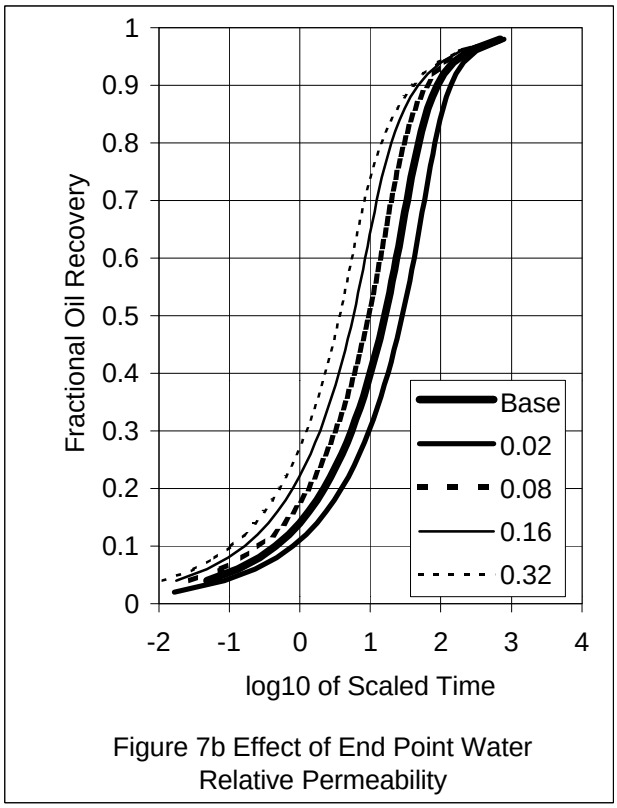

Figure 7b Effect of End Point Water Relative Permeability

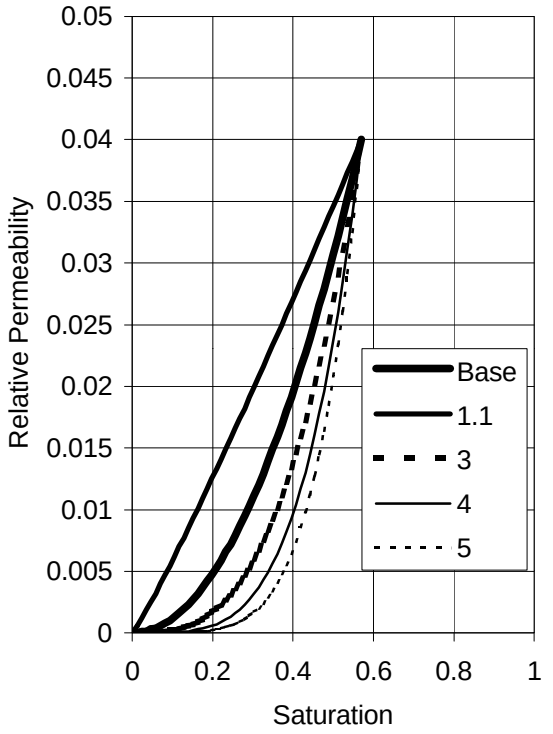

Figure 8a Water Relative Permeability Curves

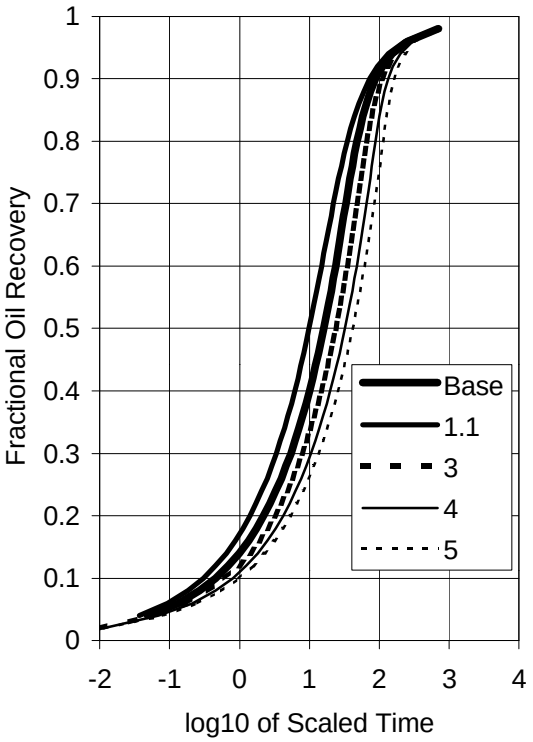

Figure 8b Effect of the Shape of the Water Relative Permeability Curve

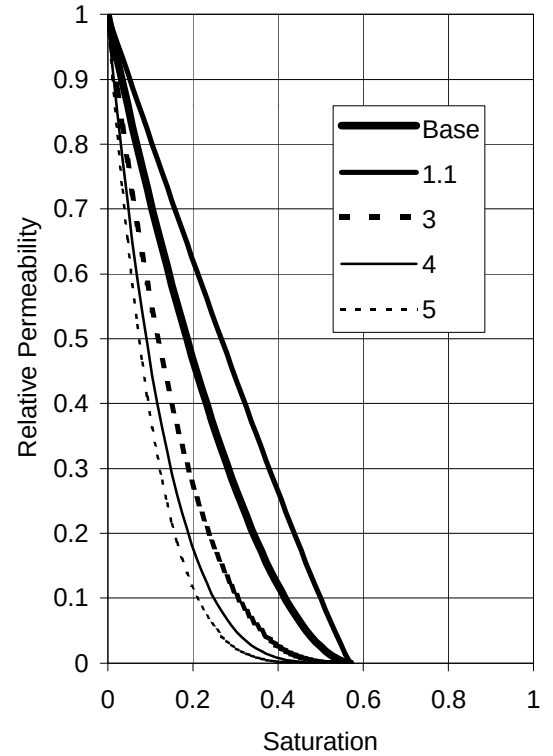

Figure 9a Oil Relative Permeability Curve

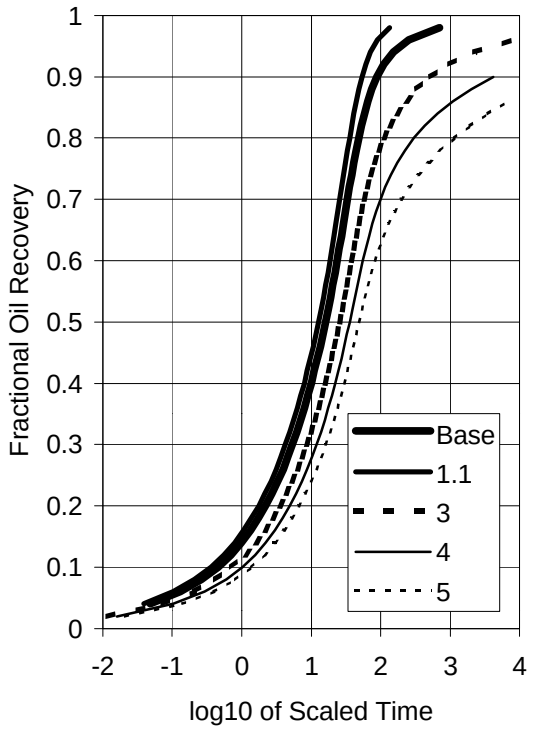

Figure 9b Effect of the Shape of the Oil Relative Permeability Curve

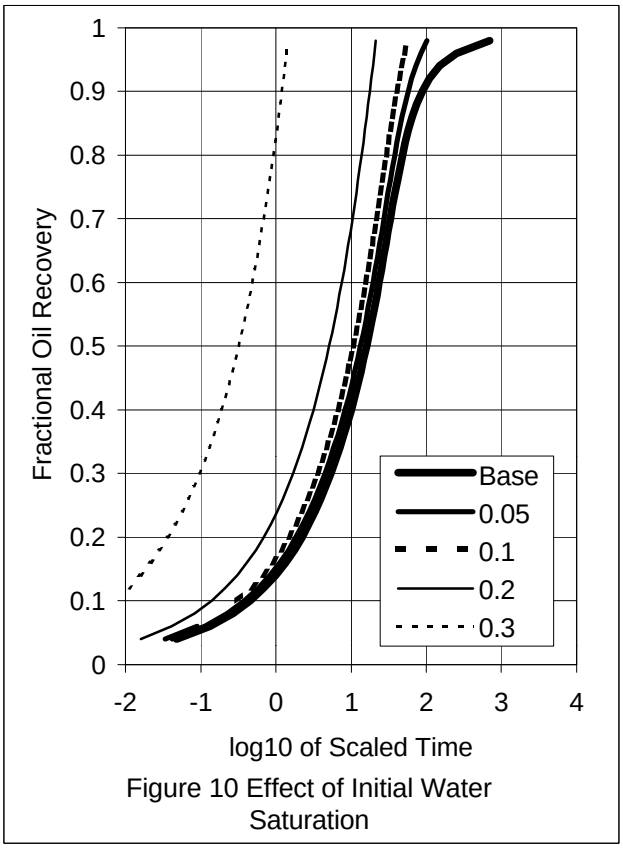

Figure 10 Effect of Initial Water Saturation

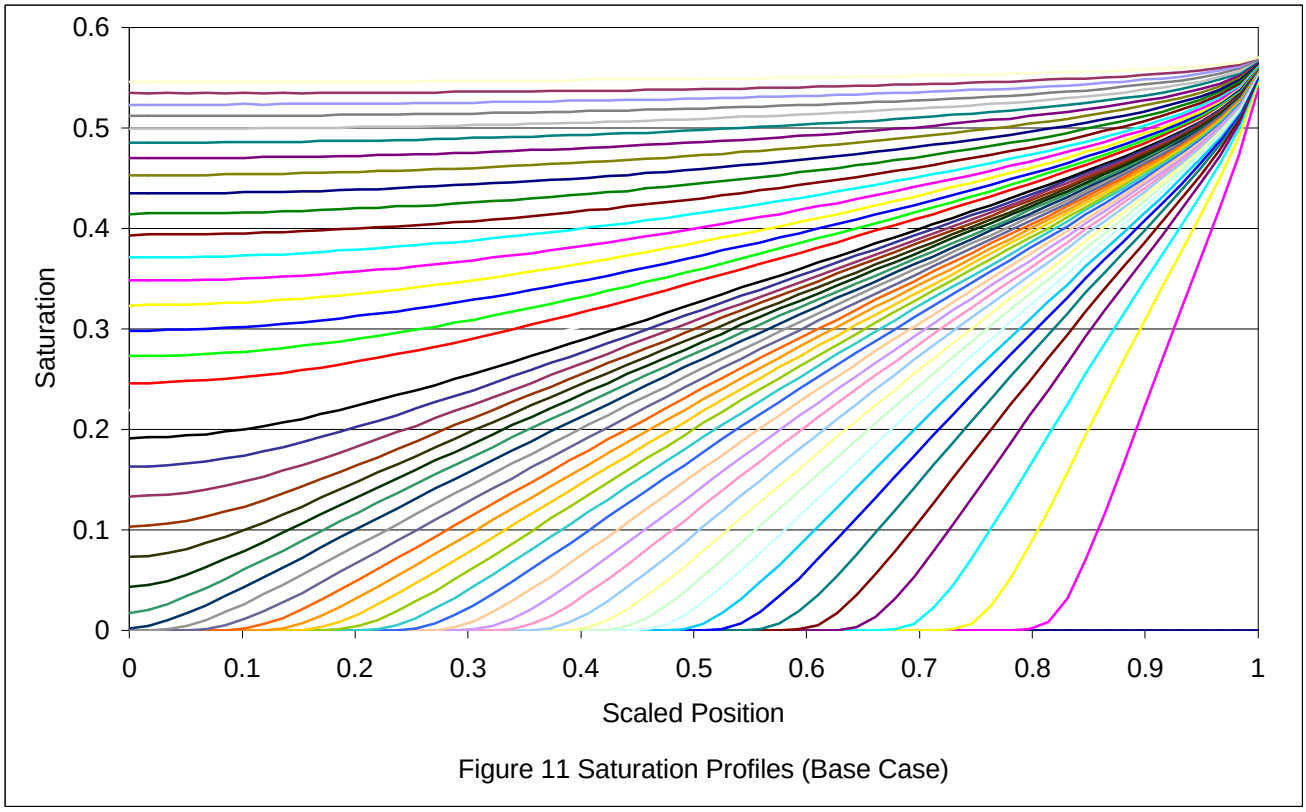

Figure 11 Saturation Profiles (Base Case)

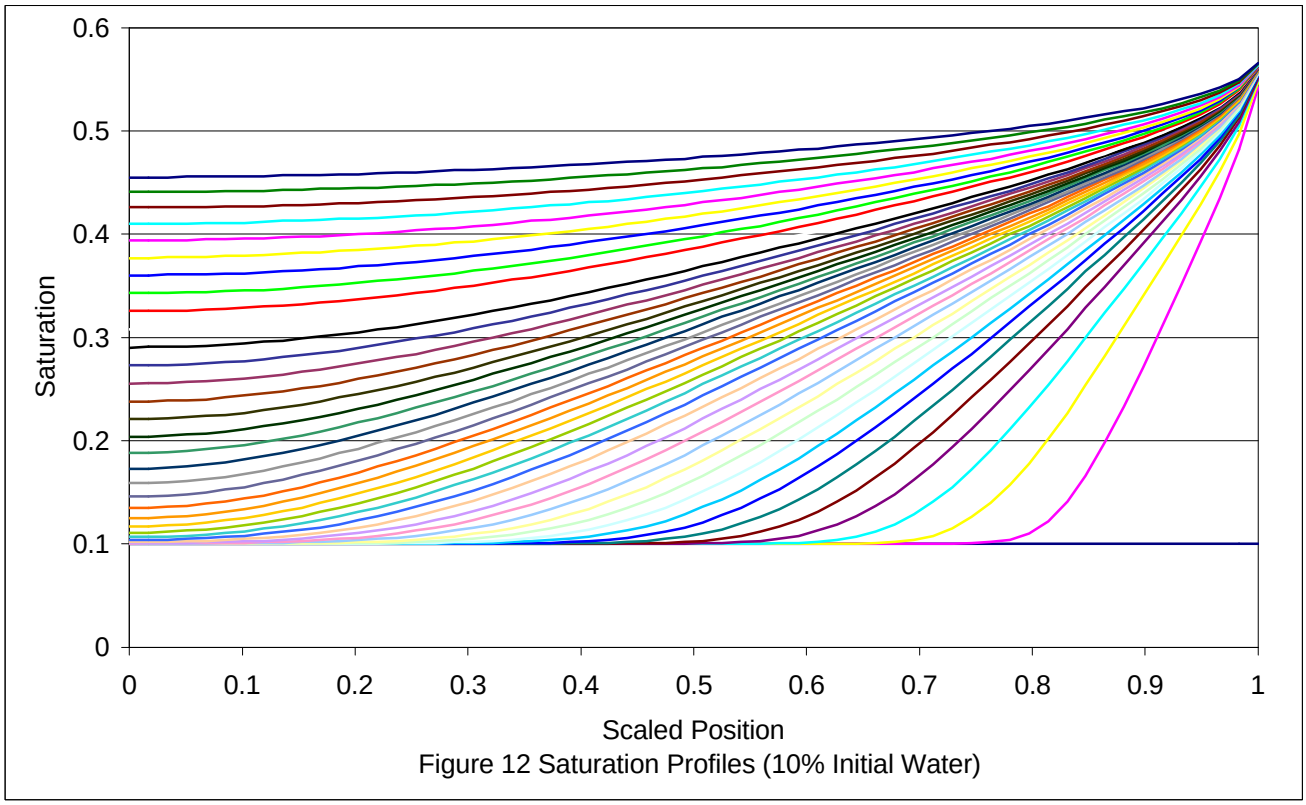

Figure 12 Saturation Profiles (10% Initial Water)